ORIGINAL PAPER

Synthesis of hybrid nanographite particles using fluidized bed system

Amitava Bhattacharyya · Mangala Joshi

Abstract Nanographite coated with ferromagnetic substances such as iron or iron oxide is a potential material for microwave absorption because of its favorable structural, magnetic, and electrical characteristics. In this paper, deposition on surfaces of acid functionalized and microwave-exfoliated nanographite particles with the use of fluidized bed system is reported. Acid functionalization improves iron adhesion and exfoliation reduces the flake thickness. The parameters influencing the deposition process are considered. It is demonstrated that Faraday's laws of electrolysis can be used for these systems if the charge transfer from solid cathode to bed particles is uniform. This requirement is satisfied only above some critical values of suspension density, electrolyte concentration, and stirring rate. The optimized values of current density are required for each specific system, as low current density leads to non-uniform deposition with local nucleation, when high a current density induces too rapid nucleation and promotes iron hydroxo complex formation. Deposition time also should be optimized for any specific system, as the expected amount of deposit cannot be formed longer because of side reactions.

Keywords Nanographite · Fluidized bed electroplating · Iron deposition

A. Bhattacharyya (✉) · M. Joshi
Department of Textile Technology,
Indian Institute of Technology Delhi,
New Delhi 110016, India
e-mail: amitbha1912@gmail.com

M. Joshi
e-mail: mangala@textile.iitd.ernet.in

Introduction

Nano-sized π-electron-based carbon materials such as fullerenes and carbon nanotubes have been intensively investigated in the recent decade because of their extensive prospects for cutting-edge nanotechnology-based devices and systems. Recently, nanographene and nanographite have been added to the family of nano-sized π-electron-based carbon materials. These materials consist of nanometer-sized graphene fragments (two-dimensional graphite) and are classified as condensed polycyclic aromatic molecules of a size extrapolated to nano-dimension [1–3]. Nanographite is a highly flexible molecular material. It exhibits electrical conductivity and high thermal conductivity in the axial direction due to the unique C–C covalent bonding. Its truncated graphene structure, as compared to bulk graphite, has more finite edge fragments. In contrast to three-dimensional fullerenes and carbon nanotubes, with their closed π-electron systems, nanographite is defined as a flat-shaped nano-sized graphene sheet featured with two-dimensional (2D) π-electron system [4].

The deposition of the iron group metals on carbon nanoparticles induces an interest because of their important mechanical and magnetic properties, which offer many industrial applications, e.g., in microsystem technologies of sensors and actuators, as microwave or radar absorbent material, and also in rocket technology, astronautics, and for anticorrosive coatings. Iron-coated multiwall carbon nanotubes were reported to be attractive electromagnetic absorbent material [5].

Currently, available methods to produce hybrid nanoparticles are sol–gel, chemical vapor deposition, physical vapor deposition, electroless coating, etc. Metal-coated hybrid nanoparticles can also be produced by electroplating of powdered nano-sized materials [6] in a fluidized bed system. This system consists of solid conducting particles

dispersed in an electrolyte, which intermittently come into contact with the solid electrode due to gravitational force (by vertical flow of electrolyte) or centrifugal force (by stirring of electrolyte). Under these circumstances the particles are polarized, and thus coated with the metallic layer [7, 8]. It was first described in 1966 and later charge transport and mass transfer in both configurations have been studied in detail. The explanation for the enhanced electron transport in these systems is mostly based on convective and conductive mechanisms [9]. The conductive mechanism requires very high number of particles as well as their collisions so that they can form chains or aggregates of particles. For convective transport of charged particles, charge sharing collisions with other particles are the most frequently considered as the reason of the enhanced electron transport. However, detailed experimental studies of the charge transport in fluidized bed systems still require the extensive studies.

A fluidized bed electrolyzer has found its applications in fuel cells, organic electrosynthesis, and metal electrowinning [10], and recently, also in fluidized bed reactors for the removal and recovery of heavy metals from aqueous solutions by bio-sorption and electrolysis. The electrolytic plating of metallic layers onto conducting micro and nanoparticles is a new area of application of the fluidized bed system. Coatings deposited in this way are of good quality, custom made, uniform, and adherent. The electrochemical deposition of a thin metal film on a primary nano filler powders may result in a product with desired properties. For a high homogeneity of the final product, every particle of the bed material should be coated uniformly by the plating metal(s).

Fluidized bed system has so far been only used to deposit nickel or cobalt on iron powder in order to prevent its oxidation. Nanographite, being a conducting nanoparticle, can be successfully used as a bed material to produce hybrid nanoparticles by coating with any metal which can be a potential microwave absorbent material. Hence, in the present study, iron deposition process on nanographite using fluidized bed system is studied, and the process parameters responsible for a good quality uniform deposition are analyzed in detail.

The efficiency of the electrolytic coating on nanographite powder is optimized by using a number of the process parameters, namely the applied current density, time, rotation rate, suspension density and average size of the particles, concentration and composition of the electrolyte, and pH. The expected iron deposition under 100% current yield is compared with the experimental (actual) yield.

Experimental

Materials

Nanographite was procured from M/s Kaiyu International (Hong Kong) with average platelet thickness of 200 nm. Analytical grade ferrous sulfate ($FeSO_4$) and ferrous chloride ($FeCl_2$) salts were supplied by Qualigen fine chemicals.

Method

Functionalization and exfoliation

Nanographite was functionalized by treating with 1:3 concentrated nitric and sulfuric acids at 38 ± 2 °C. Liquor ratio was 1:40 (*w/v*), with 1 h ultrasonication (37 KHz) and continuous stirring (600 rpm) for 24 h. Then the material was exfoliated under microwave treatment of 2.45 GHz for 60 s. The degree of functionalization was examined by Fourier transform infrared spectroscopy from Perkin Elmer. The specific surface area of functionalized and microwave-treated nanographite was measured by the BET method in Micromeritics ASAP 2010. The BET surface area of exfoliated nanographite was found to be 12.2 m^2/g, as shown in Table 1. Acid functionalized nanographite can be easily dispersed in water and promotes better surface adhesion of metal cations. This functionalized and exfoliated nanographite was used as the standard bed material for electrolytic coating.

Deposition

Iron was deposited on exfoliated and functionalized nanographite from the bath containing various concentrations of ferrous salts. For optimization of bath composition, various concentrations of both salts are taken in de-ionized water, and solution resistance and pH are measured. The constant value of bath resistance between anode and solid cathode (escaping further decrease with salt concentration) is considered as the minimum amount of salt required for the process.

Table 1 BET surface area, pore volume, and diameter of nanographite and exfoliated nanographite

Sample	Surface area (m^2/g)	Pore volume (cm^3/g)	Pore diameter (Å)
Nanographite	8.8 ± 0.2	0.08	379 ± 8
Microwave-treated functionalized nanographite	12.2 ± 0.2	1.09 ± 0.01	$3,575 \pm 71$

After optimization of the bath composition, freshly prepared 0.1 M $FeCl_2$ solution in de-ionized water (solution pH 2.9 at 30 °C) was used as a standard bath to study the effects of all other process parameters. De-ionized water was de-aerated for 30 min prior to solution preparation using nitrogen gas, and the gas flow was also maintained through the electrolyte bath during deposition. During deposition, the temperature in the electrolytic cell was kept constant at 38±2 °C. The fluidized bed system was arranged by circular stirring of the electrolyte suspension at a stirring rate of 100, 500, or 1,000 rpm. The values of the nanographite powder added into 200 ml of electrolyte were from 0.10 to 1.0 g. The electrolysis was carried out for 15, 30, 60, and 90 min. The current density was varied in the range 0.02–0.4 A/m^2.

The electrolytic cell was designed to achieve the maximum cathode contact with the bed particle by introducing a stainless steel wire net cylindrical cathode and an iron rod anode at center of cathode (see Fig. 1). The total surface area of wire net cathode immerged in the bath was calculated as 0.01 m^2 (wire diameter being 340 μm and total length of wire being 9.7 m). Functionalized nanographite was dispersed in the electrolyte solution by introducing magnetic stirrer, but after iron deposition a portion of the coated particles is accumulated on the surface of the magnetic stirrer. After deposition process the nanoparticles are filtered through Millipore vacuum filter with 0.2 μm Teflon filter. The filtrate was washed twice with de-ionized water and dried at 120 °C for 4 h in vacuum. The amount of metal deposited on the nanoparticles was found out by measuring its weight.

The efficiency of this process (η_{pow}) can be derived by the following equation [7]:

$$\eta_{pow} = \frac{\%_{Me}(\text{act.}) \times 100(\%)}{\%_{Me}(\text{calc.})} \quad (1)$$

In the present study, the actual amount of deposited iron percentage $\%_{Me}(\text{act.})$ as related to the total weight of metal

deposited nanographite powder was found by measuring the weight of the coated particles.

From Faraday's law of electrolysis, the expected amount and percentage of metal deposited on powder particles, i.e., $\%_{Me}(\text{calc.})$, may be calculated according to the Eqs. 2a and 2b:

$$m_{Me}(\text{calc.}) = \frac{Q_{pow}(\text{calc.}) \, I \, t \, M_{Me}}{Z \, F} \quad (2a)$$

$$\%_{Me}(\text{calc.}) = \frac{m_{Me}(calc.) \times 100(\%)}{m_{Me}(\text{calc.}) + m_{pow}} \quad (2b)$$

I and t represent the current passing through the cell and the electrolysis time, respectively, M_{Me} is the molar mass of the metal for coating, Z is the valency number of ion of the metal, being 2 for ferrous salt, and F is the Faraday constant. Faraday constant=96485.34 s A/g* equivalent and molar mass of iron 55.85 g/mol.

The $Q_{pow}(\text{calc.})$ is the dimensionless amount of charge on the powder particles as the fraction of the surface area of powder particles which is:

$$Q_{pow}(\text{calc.}) = S_p/(S_{cath} + S_p) \quad (3)$$

S_{cath} is the geometrical surface area of the solid cathode and S_P is the total surface area of the powder present in the volume of the electrolyte suspension in contact with the cathode. In the present study, the cathode design is changed to maximize the surface area of nanographite attached to cathode; however, the surface area of exfoliated nanographite (12.2 m^2/g) is very high as compared to a solid cathode (0.01 m^2), especially at high suspension densities, which means $S_P \gg S_{cath}$. Therefore, the relative amount of charge $Q_{pow}(\text{calc.})$ is assumed to be close to one, and the current density is calculated by dividing directly the total current to specific surface area (m^2/g) and mass of nano-

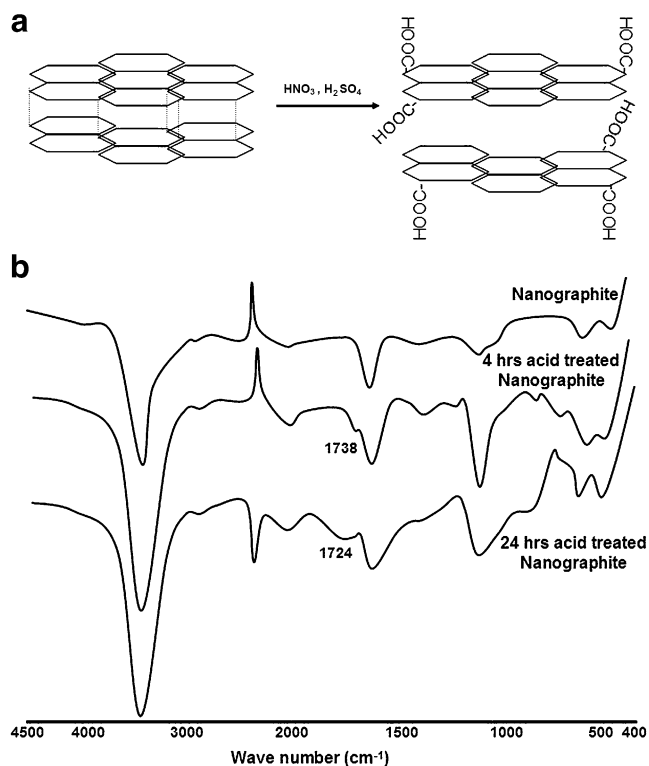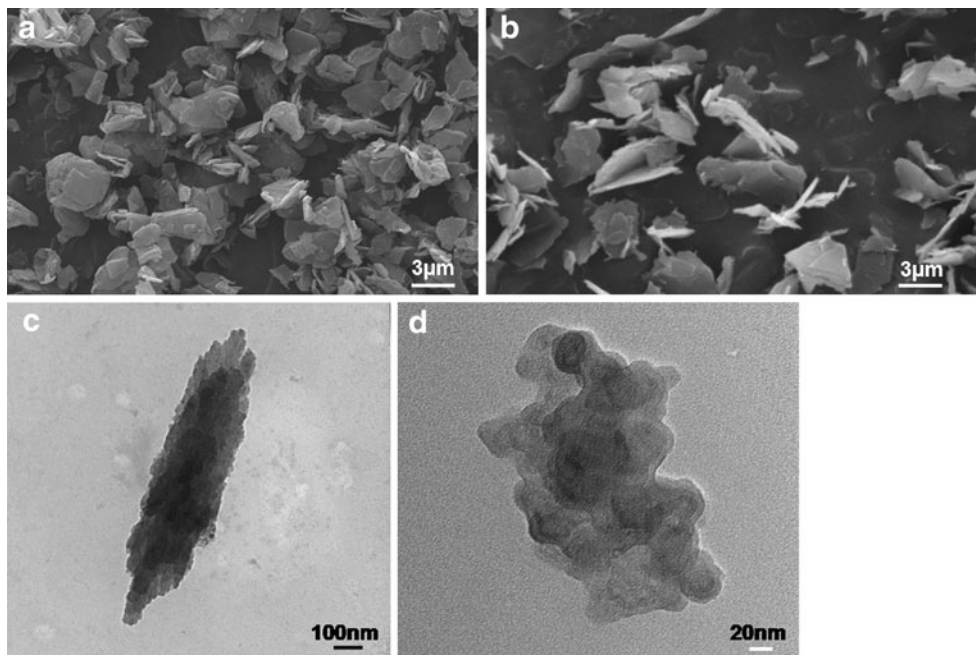Fig. 1 Schematic diagram of electrolytic cell; a side view, b top view
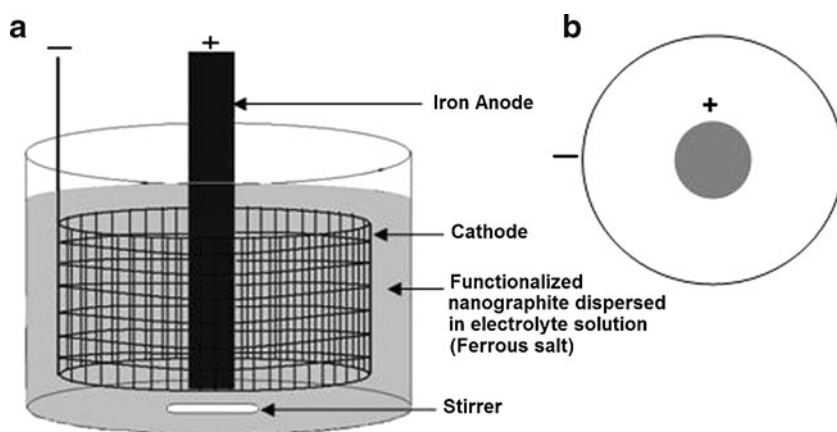
Fig. 2 **a** Reaction scheme for functionalization of nanographite and **b** FTIR curve demonstrating a new peak at 1,724 cm^{-1} for functionalized nanographite, due to –COOH group formation

graphite (g) added, i.e., with respect to powder surface area S_P. So, the Eq. 2a is modified as:

$$m_{Me}(calc.) = \frac{I\,t\,M_{Me}}{Z\,F} \tag{4}$$

It can be inferred from Eq. 4 that under continuous charge transfer condition from solid cathode to bed particles, the amount of deposited iron is directly proportional to the current and the time of deposition only. However, the critical values of the stirring rate and the concentration of bed material must be found out for any system, which support the uniform charge transfer between solid cathode and bed particles.

Characterization

Cathode ray oscilloscope from Kikusui Electronic Corp. Japan (COR 5561U) was used to observe steady charge transfer conditions from solid cathode to bed particle. SEM and EDX studies were carried out in Zeiss EVO 50. The amount of deposited metal was assessed through EDX quantitative analysis. The thermo gravimetric analysis (in Perkin Elmer TGA-7) was carried out to find the metal oxide residue after the nanoparticles charring in air, with a scan rate of 20 °C/min in 50–900 °C interval. Pan Analytical Wide angle X-ray machine (X'Pert PRO, Ni filtered CuKα radiation) was used to register the X-ray patterns of the powdered particles. TEM images have been taken in Philips CM12.

Results and discussion

Effect of functionalization and exfoliation

Nanographite is intercalated and functionalized with a mixture of 1:3 nitric acid and sulfuric acid (concentrated). The
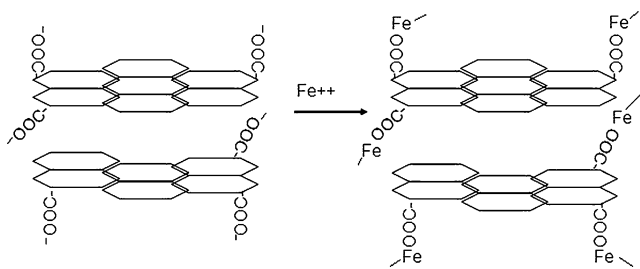
Fig. 3 SEM images of **a** nanographite and **b** exfoliated nanographite and TEM images of **c** nanographite and **d** exfoliated nanographite

Fig. 4 Reaction scheme of functionalized nanographite interaction with ferrous ion

functionalization process results in generation of –COOH groups at nanographite surfaces (Fig. 2a). At least 24 h period of acid treatment is required to functionalize the nanographite, as observed by means of FTIR study (Fig. 2b). After 4 h treatment a small peak is observed at 1,738 cm^{-1}, which becomes significant after 24 h of treatment. This peak confirms the presence of –COOH group on nanographite.

The application of 60 s microwave treatment results in successful exfoliation, as both the surface area and pore volume and diameter increase as compared to procured nanographite flakes (Table 1). SEM and TEM images confirm that the nanographite flakes become sufficiently thin, giving a possibility to deposit metal on submicron size nanographite particles (Fig. 3).

This functionalized and exfoliated nanographite is used as a bed material for the fluidized bed system. Iron (Fe^{++}) from the electrolyte solution can be attached to functional group (–COOH), so even in the absence of current applied to the system a small amount of iron is bound, as observed in EDX experiments. This was not the case for non-functionalized nanographite without polarization. Lowering pH from 2.9 to 2.5 after preparation of 2.5 g l^{-1} functionalized nanographite suspension in 0.1 M FeCl$_2$ solution indicates generation of H$^+$, as proposed in the reaction scheme.

However, the iron bound to functionalized nanographite (Fig. 4) is not crystalline if no electroplating current is applied. This is found by means of X-ray study of bed material, intermediate, and final products (see Fig. 5). The presence of some products on the nanographite surface is evident from the decrease in intensity of the peaks in Fig. 5 (a–c). The peaks observed in the X-ray patterns of exfoliated nanographite, iron-deposited nanographite after treatment under open circuit (i.e., in 0.1 M FeCl$_2$ solution after 60 min stirring), iron-coated nanographite at standard electrolysis condition of 0.3 A/m^2 current density for 60 min (in 0.1 M FeCl$_2$ solution) in air and under nitrogen atmosphere are listed in Table 2. These peaks are assigned to various crystalline phases according to the Joint Committee on Powder Diffraction Standards database (JC PDS card). The [110] peak of Fe is overlapped with [101] peak of graphite. In Fig. 5a, the [200] and [211] peaks of pure iron are observed at 65° and 82.3°, respectively, when both are absent in Fig. 5c. This confirms that the crystalline iron is formed only under electroplating conditions. However, when the deposition is carried out in air, the presence of two characteristics peaks at 35.6° and 62.8° (pattern b in Fig. 5) confirms the presence of iron oxide on the surface of nanographite. As nano-crystalline iron is strongly reactive [11], the deposited iron reacts with atmospheric oxygen to form iron oxide on top of the deposited layer.

The TGA curves of iron deposited on functionalized and non-functionalized nanographite (Fig. 6) reveal that despite of significant amount of metal deposited in both cases the non-functionalized sample demonstrates the original nanographite curve, i.e., the two phases are observed separately, while for functionalized material the weight loss is gradual. So, the functionalization supports more effective deposition of pure iron on the surface of nanographite and improves the adhesion between nanographite and the deposits. The residue is almost 7% higher than the amount measured by weighing the deposited nanographite. This is because of the metal oxide formation during TGA in air.

Fig. 5 X-ray patterns for *a* iron-deposited nanographite under nitrogen atmosphere; current density, 0.3 A/m^2; FeCl$_2$ concentration, 0.1 M; time, 60 min; 1,000 rpm. *b* Iron-deposited nanographite in air; current density, 0.3 A/m^2; FeCl$_2$ concentration, 0.1 M; time, 60 min; 1,000 rpm. *c* Iron-deposited nanographite under open circuit conditions; FeCl$_2$ concentration, 0.1 M; time, 60 min; 1,000 rpm. *d* exfoliated nanographite
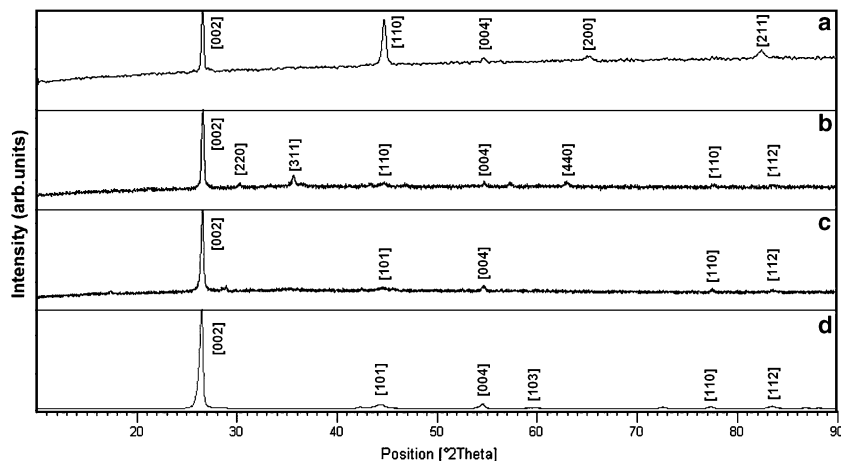
Table 2 Major X-ray peaks as observed in Fig. 5

Peak (2θ degree)	Miller indices	Contribution	JC PDS no.
26.5	002	Nanographite (curve a, b, c, d)	41-1487
30	220	Iron oxide–magnetite (curve b)	19-0629
35.6	311	Iron oxide–magnetite (curve b)	19-0629
44.4	101	Nanographite (curve a, b, c, d)	41-1487
44.6	110	Iron (curve a, b)	06-0696
54.6	004	Nanographite (curve a, b, c, d)	41-1487
59.7	103	Nanographite (curve d)	41-1487
62.8	440	Iron oxide–magnetite (curve b)	19-0629
65	200	Iron (curve a)	06-0696
77.3	110	Nanographite (curve b, c, d)	41-1487
82.3	211	Iron (curve a)	06-0696
83.3	112	Nanographite (curve b, c, d)	41-1487

Effect of electrolyte composition

Electrolyte provides the conductivity of the system, and eventually increases the current density at a given voltage. Thus, its concentration favors the higher amount of deposit formed on the bed particle. In order to measure the resistance, a multimeter is connected between anode and solid cathode of the deposition bath containing de-ionized water and then the salt is added gradually into the bath.

After achieving a certain value of electrolyte concentration the pH and conductivity of the system remain almost constant, as observed in Fig. 7. $FeCl_2$, 0.1 M, is found to be a minimum concentration for successful deposition process. Thus, 0.1 M $FeCl_2$ solution is used as a bath in all subsequent experiments.

Addition of hydrochloric acid (HCl) to the electrolyte solution results in further resistance decrease, and thus the current density may further increase. However, in practice
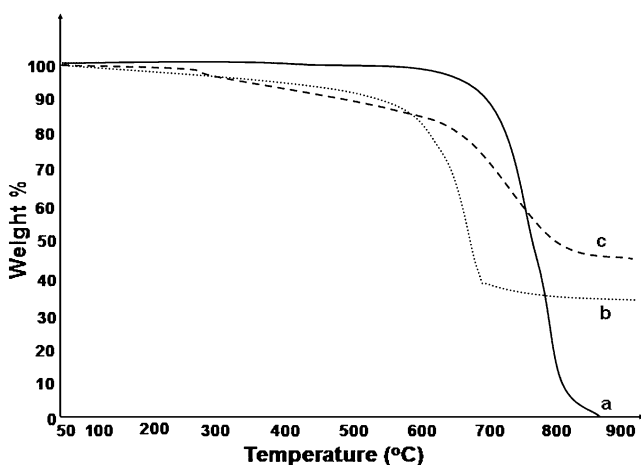
very small amount of HCl reduces the pH drastically and very low amount of iron is deposited, as the dissolution of the deposited iron happens and parallel hydrogen evolution takes place. As usually, electrodeposition from aqueous electrolytes presents simultaneous discharge of metal and hydrogen cations. The rates of these parallel reactions vary according to the electrolyte composition and cathode
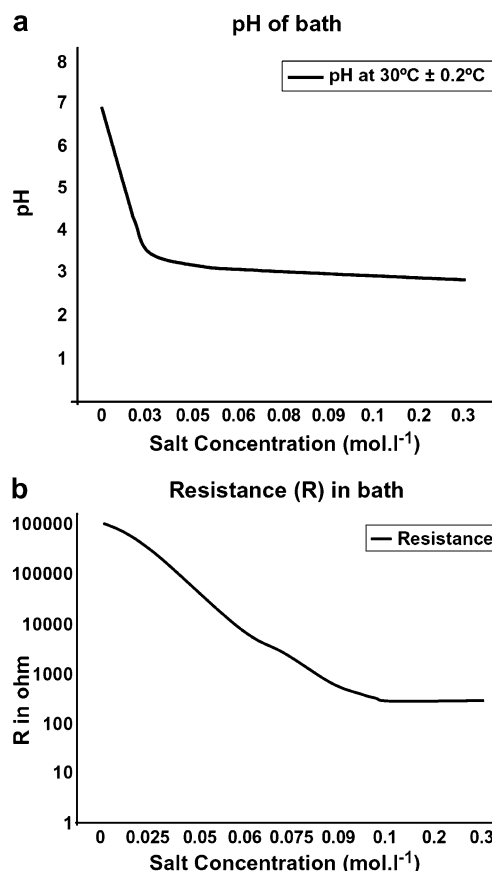

Fig. 6 TGA in air of *a* nanographite, *b* iron-deposited non-functionalized nanographite, and *c* iron-deposited functionalized nanographite; deposition condition: current density, 0.35 A/m²; $FeCl_2$ concentration, 0.1 M; time, 30 min; 1,000 rpm in both (*b*) and (*c*)

Fig. 7 The effect of electrolyte ($FeCl_2$) concentration on **a** pH and **b** resistance of the bath

Table 3 EDX quantitative analysis for iron-coated nanographite synthesized using two different types of electrolytes; current density, 0.3 A/m^2; ferrous salt concentration, 0.1 M; time, 60 min; and 1,000 rpm

Element	wt.% Chloride salt bath	wt.% Sulfate salt bath
Carbon	47.87	28.87
Iron	27.85	38.91
Silicon	0.5	0.24
Sulfur	0.16	1.3
Chlorine	0.1	0
Chromium	0.41	0.39
Oxygen	23.12	30.3

potential. Additional problem with the iron salt is the tendency to form hydroxides [12], which is more pronounced for Fe(3+). Ferrous salts were used in the present study, as the presence of trivalent iron reduces the current efficiency. However, the chance of oxidation of ferrous solution by the atmospheric oxygen increases with time. The use of HCl also increases the chance of oxidation of ferrous ion and in due course, it may lead to breakdown of the entire electrodeposition process. This is the reason why HCl is not further used in our experiments as a standard electrolyte bath.

In the present study, two types of salts, i.e., FeCl$_2$, FeSO$_4$ (0.1 M solution in each case) were used for iron deposition. Table 3 summarizes the weight percentage (wt. %) of the elements in iron-coated nanographites produced from these two baths. A small amount of chromium and silicon detected in the EDX quantitative analysis may appear due to the impurity present in the iron anode.

The presence of oxygen even when deposition takes place from chloride bath indicates the extent functionalization of nanographite (–COOH group formation). The

sulfate salt demonstrates the problem of residual sulfur content, which is prone to atmospheric degradation in the course of coating applications, so its use is not further recommended. The solubility of sulfate salt is lower as compared to chloride salt, so the removal of sulfate salt from the coating is also more difficult. The higher amount of sulfur and oxygen indicates the presence of FeSO$_4$ in iron-coated nanographite produced from sulfate bath.

Effect of stirring speed

Basically, there should be no effect of the stirring rate under a steady charge transfer conditions. To check this statement, a simple experiment was carried out with the help of cathode ray oscilloscope. Of nanographite, 0.5 g was added to the 200 ml 0.1 M electrolyte solution. Due to the intermittent contact of bed particle with solid cathode, a fluctuating voltage is observed at low stirring rate. With its increase from 100 to 1,000 rpm the charge transfer from solid cathode to bed particle (nanographite in this case) becomes uniform, and thus the amplitude fluctuations gradually go down (Fig. 8). Amplitude fluctuations were also observed at the anode.

However, the uniform behavior can be also achieved at lower rounds per minute when high concentration of bed material is used. The shape of cathode is another factor affecting the uniform charge transfer in the system. In the present system, anode is positioned just at the center of the cylindrical cathode, and centrifugal force induced by stirring is utilized for charge transfer to nanographite from solid cathode. The shape of cathode and its constant distance from the anode helps to stabilize the system at low concentration of bed particle. Whenever the fluidized bed system is used to deposit metal on the particles, it is absolutely necessary to find out the uniform charge transfer condition to have a uniform coating on bed particles.

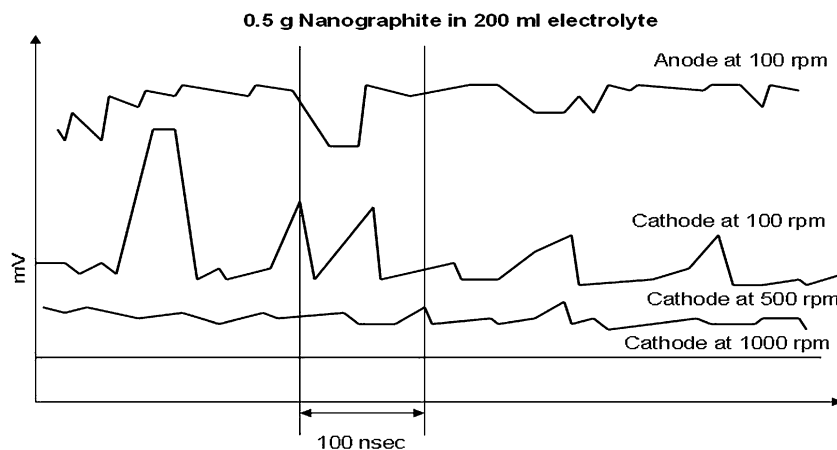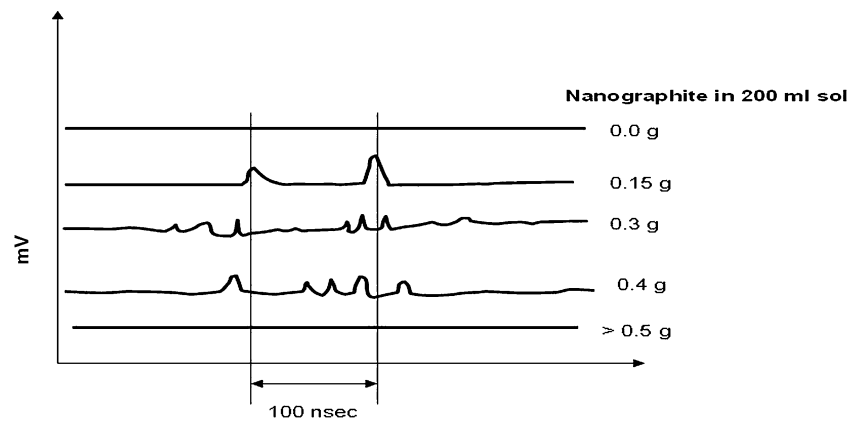**Fig. 8** Cathode ray oscilloscope response profile at cathode and anode at different stirring rate

Nanographite in 200 ml sol

0.0 g

0.15 g

0.3 g

0.4 g

> 0.5 g

mV

100 nsec

Effect of particle concentration

The steady state can be achieved with increase in particle concentration, as it was already stated in the earlier section. It has been observed that at 1,000 rpm at least 0.5 g of nanographite is needed for 200 ml of solution and the specific type of cathode we used to provide a uniform charge transfer (Fig. 9). The cathode voltage profile with the addition of nanographite indicates that at very low concentration the charge transfer is non-uniform. The uniform deposition of iron takes place if the concentration is above a minimum value for which any noise in the system is absent. In the system used in this study, a minimum value of 2.5 g l^{-1} nanographite suspension is needed to avoid the unevenness of the coating. Keeping all other parameters the same, the amount of metal deposited is increased with nanographite concentration. The effect is less noticeable above already
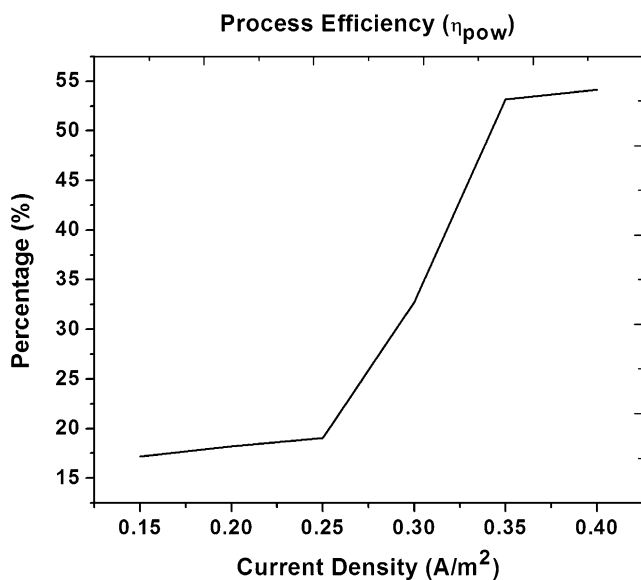
mentioned value of 2.5 g l^{-1}. For micron size particles, the effect of particle concentration on deposition is more pronounced, as the available surface area in contact with cathode is greatly increased with concentration [13]. At the same time, for nanoparticles their interaction with solid cathode is excessive, even at low concentration. Moreover, too high concentration leads to decrease in the amount of deposited metal, may be due to formation of conducting path from anode to cathode through the bed particle, which is surely undesirable. We found that no more than 1 g of nanographite can be introduced into the 200 ml bath.

Electroplating efficiency

The electroplating efficiency (η_{pow}), i.e., the amount of iron deposited on bed material with respect to the expected amount of metal (considering 100% current yield) is an important factor. η_{pow} is the efficiency of the process calculated from Eq. 1. The actual amount of deposited iron percentage, i.e., %$_{\text{Me}}$(act.) on the total weight of metal-deposited nanographite powder, was obtained by weighing directly the bed material before and after 30 min deposition.
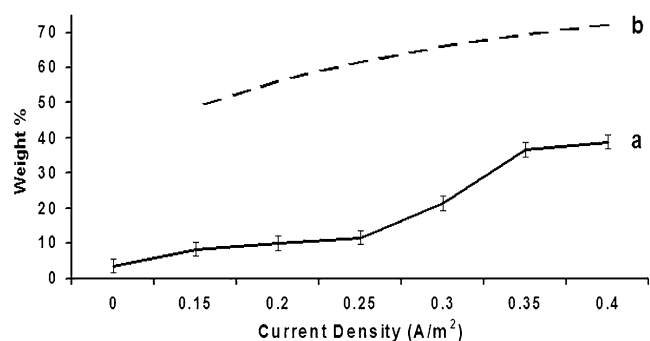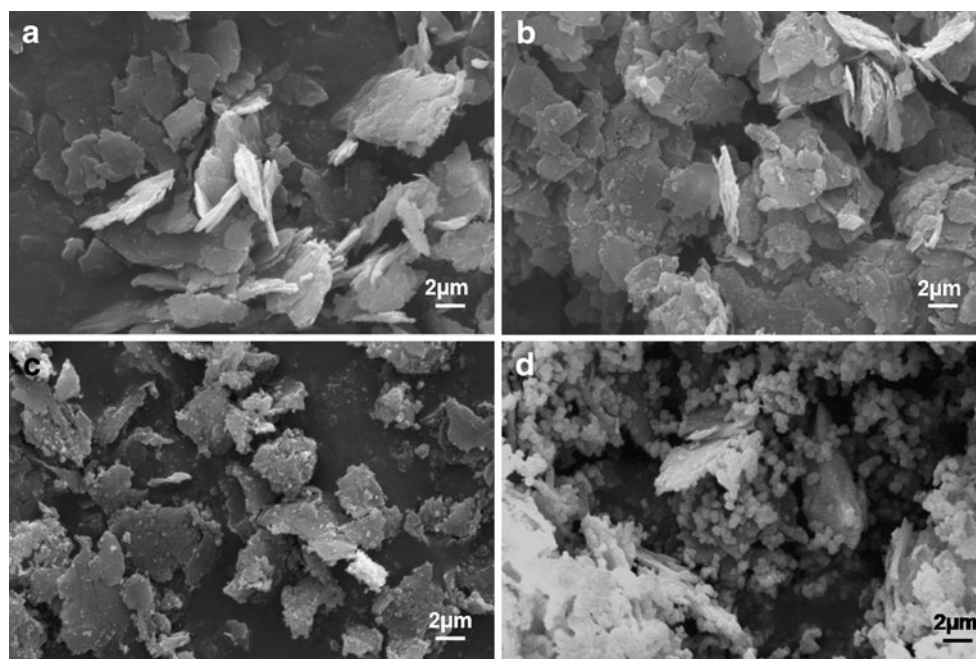

Process Efficiency (η_{pow})

Fig. 10 Process efficiency η_{pow} (according to Eq. 1) at different current densities; FeCl$_2$ concentration, 0.1 M; functionalized nanographite added, 0.5 g; time, 30 min; 1,000 rpm

Fig. 11 *a* The weight percentage of deposit %$_{\text{Me}}$(act.) on total weight of particles after deposition at different current densities and *b* expected deposit %$_{\text{Me}}$(calc.) (according to Eq. 2b and Eq. 4) on total weight of particles after deposition at corresponding current densities; FeCl$_2$ concentration, 0.1 M; functionalized nanographite added, 0.5 g; time, 30 min; 1,000 rpm

Fig. 12 Iron-deposited nanographite at different current densities **a** at 0.02 A/m², **b** at 0.2 A/m², **c** at 0.35 A/m², and **d** rapid nucleation at 0.40 A/m²; FeCl₂ concentration, 0.1 M; functionalized nanographite added, 0.5 g; time, 30 min; 1,000 rpm

This amount is confirmed by using SEM/EDX quantitative analysis. Figure 10 shows the efficiency of the process (η_{pow}) increase with current density. Initially, it is very poor, but it attains some higher value with the increase in current density, slightly exceeding 50%. The reasons may be the charge loss in the contact with anodes and slow iron complex formation reactions.

Effect of current density

The weight% of deposit on total weight of coated nanographite particles, i.e., %_{Me}(act.), after 30 min of electrodeposition at various current densities is shown in Fig. 11. The amount of iron was confirmed with EDX quantitative analysis. The amount of iron deposited increased with the current density as expected. The initial deposition is attributed to the functionalization of nanographite. Starting from a certain value of current density (0.25 A/m²), the deposition became more efficient, but further increase in current density could not help much in deposition. As the deposition time (30 min) and amount of bed particle (0.5 g) is constant in each case, the current density is equivalent to the total charge. So, it can also be stated that the amount of deposit is not linearly increased with the total charge as expected from Eq. 4 considering 100% current yield.

SEM images show that nanographite surface gets covered with the deposited iron as the current density increases. At low current density the coating is non-uniform, but some features of local nucleation are observed after prolonged deposition (Fig. 12a). At high current density, the coating uniformity, as well as high amount of deposit, can be achieved (Fig. 12b). However, the higher current density leads to uneven

deposition (Fig. 12c), which may not be desirable for some applications. At the same time, applications like microwave absorption requires less uniform surface. Even higher current density leads to rapid nucleation (Fig. 12d), and the coating quality appears to be very poor. We can conclude that low to moderate current density interval is favorable for uniform deposition on nanographite surface.

Effect of time

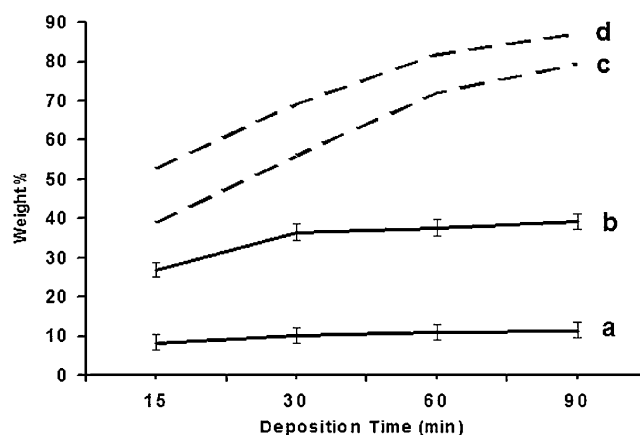The electrolysis time is an important parameter which strongly influences the electrodeposition of metals. Of

Fig. 13 The dependence on electroplating time of experimental deposited iron (as weight% on weight of iron-coated nanographite) at *a* 0.2 A/m², *b* 0.35 A/m² current densities and calculated amount of deposited iron (according to Eq. 2b and Eq. 4) at *c* 0.2 A/m², *d* 0.35 A/m² current densities; FeCl₂ concentration, 0.1 M; functionalized nanographite added, 0.5 g; 1,000 rpm

course, the total amount of the deposited metal and the final thickness of the coating layer are expected to increase with deposition time. The weight% of deposit related to total weight of iron-coated nanographite particles at two different current densities and the corresponding expected deposition trend are shown in Fig. 13.

As expected from Eq. 4, the deposition is increased with time when the current (current density and amount of bed particle) is constant; however, the increase is not so great. The effect of time on deposition is less at low current density (0.2 A/m^2). At high current density (0.35 A/m^2), the rate of increase is initially high but after some time the deposition rate is reduced. This may be due to the formation of iron hydroxo complexes via aqueous hydrolysis of iron salt [7]. Thus, it can be concluded from the curve that the high current density (>0.2 A/m^2) and a time of 30 min is found to be suitable for iron deposition in the system used in this study.

Conclusions

The process parameters hold the key for the successful deposition of metal on nanographite particles using fluidized bed system. Above some critical value of stirring rate, bed particle, and electrolyte concentration, uninterrupted and efficient mass and charge transfer to bed particles occurs. However, at low current density the process efficiency is very poor. The expected amount of iron deposit (below 100% current yield) could not be achieved at longer time, as the hydrogen evolution and hydroxo complex formation may dominate at later stages. Although a high current density over a short period gives higher deposition efficiency, but too high current density results in a rapid nucleation on nanographite surface, which in turn causes uneven deposition.

Iron-coated nanographite produced by this method is a potential light weight hybrid nanomaterial suitable to develop microwave adsorbent nanocomposite coatings and laminates on fabrics or nets. Such fabrics can find potential use in several defense applications, such as specialty coatings for camouflage covers, nets, and other coated textiles used for aerial surveillance, etc. The top surface layer of iron-deposited nanographite is prone to oxidation on exposure to air. To overcome this drawback, the studies on iron nickel co-deposition are in progress and will be reported in our next publication.

References

1. Goto K, Kubo T, Yamamoto K, Nakasuji K, Sato K, Shiomi D, Takui T, Kubota M, Kobayashi T, Yakusi K, Ouyang J (1999) J Am Chem Soc 121:1619–1620
2. Fukui K, Sato K, Shiomi D, Takui T, Itoh K, Gotoh K, Kubo T, Yamamoto K, Nakasuji K, Naito A (1999) Synth Met 103:2257–2258
3. Inoue J, Fukui K, Kubo T, Nakazawa S, Sato K, Shiomi D, Morita Y, Yamamoto K, Takui T, Nakasuji K (2001) J Am Chem Soc 123:12702–12703
4. Chen SC, Lin CY, Lin MF (2008) Diamond Relat Mater 17:1545–1549
5. Shen X, Gong RZ, Nie Y, Nie JH (2005) J Magn Magn Mater 288:397–402
6. Griego TP, Eichman JW (2005) U S Patent B2:6,942,765
7. Galova M, Orinakova R, Lux L (1998) J Solid State Electrochem 2:2–6
8. Turonova A, Galova M, Supicova M (2003) J Solid State Electrochem 7:684–688
9. Orinakova R, Wiemhofer HD, Paulsdorf J, Barinkova V, Bednarikova A, Smith RM (2006) J Solid State Electrochem 10:458–464
10. Shvab NA, Stefanjak NV, Kazdobin KA, Wragg AA (2000) J Appl Electrochem 30:1285–1292
11. Guo L, Huang Q, Li X, Yang S (2001) Phys Chem Chem Phys 3:1661–1665
12. Gladkikh SN, Gladkikh YN (1995) Chem Pet Eng 31:36–38
13. Turonova A, Galova M, Supicova M, Lux L (2003) J Solid State Electrochem 7:689–693